Dalton Transactions

Accepted Manuscript

This article can be cited before page numbers have been issued, to do this please use: K. Durka, M. Urban, M. Czub, M. Dbrowski, P. Tomaszewski and S. Lulinski, *Dalton Trans.*, 2018, DOI: 10.1039/C7DT04858K.

ROYAL SOCIETY OF CHEMISTRY

rsc.li/dalton

View Article Online
DOI: 10.1039/C7DT04858K

Intramolecular ortho-Assisted Activation of Silicon-Hydrogen Bond in Arylsilanes: An Experimental and Theoretical Study

Krzysztof Durka,[a,*] Mateusz Urban,[a] Maja Czub,[a] Marek Dąbrowski,[a] Patryk Tomaszewski,[a] Sergiusz Luliński[a,*]

[a]*Department of Physical Chemistry, Faculty of Chemistry, Warsaw University of Technology, Noakowskiego 3, 00-664 Warszawa, Poland*

Abstract

Intramolecular activation of the Si–H bond in arylsilanes by selected *ortho*-assisting functional groups based on boron, carbon and phosphorus was investigated experimentally and by means of theoretical calculations. The major conclusion drawn is that the presence of negatively charged oxygen atom in the functional group is essential for providing effective chelation to the silicon atom which in turn results in the increased hydridic character of a resulting five-coordinated species. In contrast, an intermolecular attack of hydroxide on the silicon atom in aryldimethylsilane results in the activation of the silicon-aryl bond. This increased reactivity of Si–H bond in intramolecularly coordinated arylsilanes can be ascribed to a significant trans effect which operates in the preferred configuration. Hydrolytic cleavage of the Si–H bond results in dihydrogen elimination and formation of various silicon heterocyclic systems such as benzosiloxaboroles, spiro-bis(siloxa)borinate, benzosilalactone and benzophosphoxasilole. In addition, intermolecular reduction of benzaldehydes with ortho-boronated arylsilane was observed whereas compounds bearing other reducible functional groups (COMe, COOEt, CN, NO_2) were inert under comparable conditions. Specifically, an intramolecular reduction of the CN group in an *ortho*-silylated benzonitrile derivative was observed. The mechanism of Si–H bond activation was investigated by the DFT theoretical calculations. They showed that the intramolecular coordination of silicon atom effectively prevents the cleavage of Si-aryl bond. Furthermore, the reaction is favored in anionic systems bearing COO^-, $B(OH)_3^-$ or CH_2O^- groups, while in the case of neutral functional groups such as $PO(OEt)_2$ the process is much slower.

Introduction

The activation of silicon-hydrogen bond is of recent prime interest.[1] This is mainly due to the use of hydrosilylation of unsaturated substrates as a powerful synthetic tool of a wide practical importance with a special emphasis on large-scale catalytic processes performed in industry.[2] However, the majority of developed protocols is based on the use of transition metal catalysts for the Si–H bond activation and subsequent hydrosilylation of substrates bearing unsaturated carbon-carbon and carbon-heteroatom bonds such as ketones, imines and

View Article Online
DOI: 10.1039/C7DT04858K

nitriles.[3] Catalysts based on zinc, tin and aluminium have also been used.[4] Furthermore, metal-free methods involving acids, bases, alkali or tetraalkylammonium fluorides were also proposed.[5] A notable example is the recently developed catalytic system, where the Si–H bond is activated by a system comprising a strongly Lewis acidic perfluorinated phosphonium cation $[(C_6F_5)_3PF]^+$,[6] eventually leading to a good performance in hydrosilylation of ketones, nitriles and imines at room temperature. Furthermore, metal-free organo-phothocatalytic system for hydrosilylation of alkenes was also proposed.[7] Finally, in the context of our work it is especially important to note that strong organoboron Lewis acid $B(C_6F_5)_3$ acts as a highly effective hydrosilylation catalyst as shown and mechanistically studied by Piers[8] and Oestreich,[9] respectively. This was complemented by successful isolation of a borole–silane adduct,[10] which apparently can be regarded as a model intermediate. In the recent striking example used combination of $B(C_6F_5)_3/Al(C_6F_5)_3$ catalytic system for effective reduction of CO_2 to CH_4.[11] In the intramolecular version of this reaction mode, the Si–H bond can be effectively activated. In the case of *ortho*-hydrosilyl-dimesityloboronbenzene an intramolecular hydride ligand transfer from silicon to boron centers was observed. Recent developments in the field of Si–H bond activation were summarized by Tilley, Oestreich and Corey.[1]

Recently, the interest in our group has focused on benzosiloxaboroles. They can be regarded as silicon benzoxaborole congeners and therefore were considered as potential antimicrobial agents as well as receptors of biologically relevant diols. We have found that benzosiloxaboroles can be conveniently obtained by a facile intramolecular dehydrogenative condensation of arylboronic acids bearing a $SiHR_2$ group at the *ortho* position in the presence of water (**Scheme 1**).[12] In our search for novel functionalized benzosiloxaboroles we have undertaken the synthesis of derivatives bearing formyl or cyano groups attached at various positions of the benzene ring.[13] These studies resulted in the preliminary observation that the activation of the Si–H by the adjacent $B(OH)_2$ group enables reduction of the CHO group under mild aqueous conditions. The proposed initial mechanical pathway for the activation of the Si–H bond involved the intramolecular interaction with the Lewis-acid boron-based group resulting in the formation of Si–H…B bridge followed by the coordination of nucleophile to silicon centre and elimination of H_2 molecule. This is in accordance with previous findings by Kawachi on the alcoholysis of 2-(dimesitylboryl)(dimethylsilyl)benzene[14] and his later mechanistic studies on intramolecular hydride ligand transfer from hydrosilyl group to *ortho*-located dimesitylboryl group.[15] In this contribution we present our experimental and computational results on various mechanistic scenarios accounting for Si–H bond activation. We went beyond the boron case to get a more general mechanistic picture. Therefore, we studied the effect of other *ortho*-assisting groups based on carbon and phosphorus. Gratifyingly, developed methodologies allowed us to obtain new classes of silicon heterocycles including a unique spiro-bis(siloxa)borinate system and phosphoxasilole.

View Article Online
DOI: 10.1039/C7DT04858K

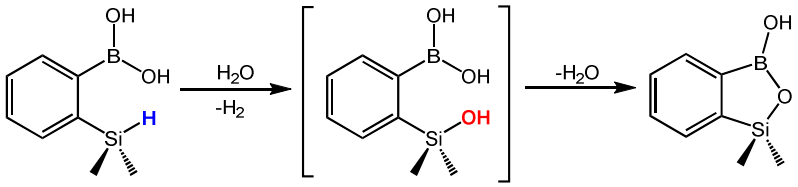

Scheme 1. Formation of benzosiloxaborole *via* boronic group-assisted activation of the Si–H bond.

Results and Discussion

Si–H bond activation with ortho-assisting boron-based groups. We have considered two general Si–H activation modes for the observed hydrosilylations. The first one relies on Lewis acid properties of the boron atom. This mechanical pathway resembles the reported activation of silicon hydrides by moderate-strong Lewis acidic dimesitylboryl group located at the vicinity of hydrosilyl group.[15] The hydride transfer from silicon to boron was also used for the preparation of some organoboron hydrides.[16] Obviously, the boron atom in $B(OH)_2$ group is not strongly Lewis acidic. Nevertheless, taking into account previous reports on related systems,[15,17] in our previous contribution we assumed that the proximity of silicon and boron centres may promote the interaction between them via hydride Si–H…B bridge formation.[12] However, to facilitate hydride migration, initial coordination of water to the silicon atom should be invoked and this is consistent with the negative entropy change. On the other hand, the presence of the boron-bound oxygen atom provides the possibility for intramolecular oxygen-silicon coordination which, in turn, may result in the Si–H bond activation. Such interaction was previously invoked to account for the reactivity of arylsilanes bearing hydroxymethyl[18] and formyl groups.[19]

We have studied the mechanism of boronic-group-assisted hydrosilylation using 1-bromo-2-(dimethylsilyl)-3-fluorobenzene **1** as a starting material. It is readily available by the deprotonative lithiation/silylation of 1-bromo-3-fluorobenzene.[12a] Compound **1** was subjected to bromine/lithium exchange with *t*BuLi/Et_2O at –90 °C to give **1-Li** which was then boronated with $B(OMe)_3$ (**Scheme 2**). The resulting suspension of the ate complex **2** was warmed to the room temperature, then evaporated and redissolved in THF. ^{10}B and ^{29}Si HMBC NMR analyses revealed the presence of a substantial amount of a aryltrihydroborate salt **3** containing the $Si(OMe)Me_2$ group ($\delta^{10}B$ = –30.6 ppm, $\delta^{29}Si$ = 12.2 ppm) resulting from the substitution of all methoxy groups at the boron atom (**Figure 1**). The spectra showed also the formation of large amounts of the boronic ate complex **4** ($\delta^{10}B$ = –0.9 ppm) as well as the neutral boronate ester **5** ($\delta^{10}B$ = 24.9 ppm), both featuring similar $\delta^{29}Si$ values (7.9 and 8.4 ppm). One can generally assume that the activation of the Si–H bond is due to nucleophilic attack of the anionic methoxy group on the silicon atom. In turn, this results in moving hydride ligands from hypervalent silicon atom to boron. Apparently, the substitution of all methoxy group at the boron atom leading to the formation of **3** is thermodynamically favoured. Treatment of the obtained mixture with ethereal HCl resulted in the rapid hydrogen evolution and conversion of **3** and **4** to **5**. The formation of hydrogen was confirmed by ^1H NMR spectrum of a mixture obtained by hydrolysis of **2** with D_2O in THF-d_8; in fact, a weak

View Article Online
DOI: 10.1039/C7DT04858K

but perceptible signal of HD was observed as a triplet (J = 42 Hz) centered at 4.48 ppm. In contrast, when **2** was quenched at –70 °C with $Si(H)ClMe_2$, the crude boronate ester **6** bearing the $Si(H)Me_2$ group ($\delta^{11}B$ = 24.0 ppm, $\delta^{29}Si$ = –17.2 ppm) resulted. This indicates that the neutral $B(OMe)_2$ group does not strongly activate the Si–H bond and the absence of an intramolecular oxygen-silicon coordination is confirmed by ^{29}Si NMR data since $\delta^{29}Si$ values for related $Si(H)Me_2$-substituted arenes are in the range of –18 - –19 ppm. A minor product of the latter reaction is presumably the related borinic derivative **7** as evidenced by the smaller ^{11}B NMR signal (ca. 8%) at 42.2 ppm. Naturally, quenching of arylboronate salt **2** or esters **5**, **6** with aqueous acids leads to condensation of B–OH and Si–OH fragments resulting in the formation of previously reported benzosiloxaborole structure **8**.[12a] However, the cleavage of Si–H bond during hydrolysis of **6** in wet THF is slow since H_2 evolution was completed only after 2-3 days. This indicates that effective activation of Si–H bond proceeds via the coordination of oxygen atom of the anionic boronate group to the silicon centre rather than intramolecular hydride transfer to boron atom (the latter mechanism operates for stronger triarylborane Lewis acids).

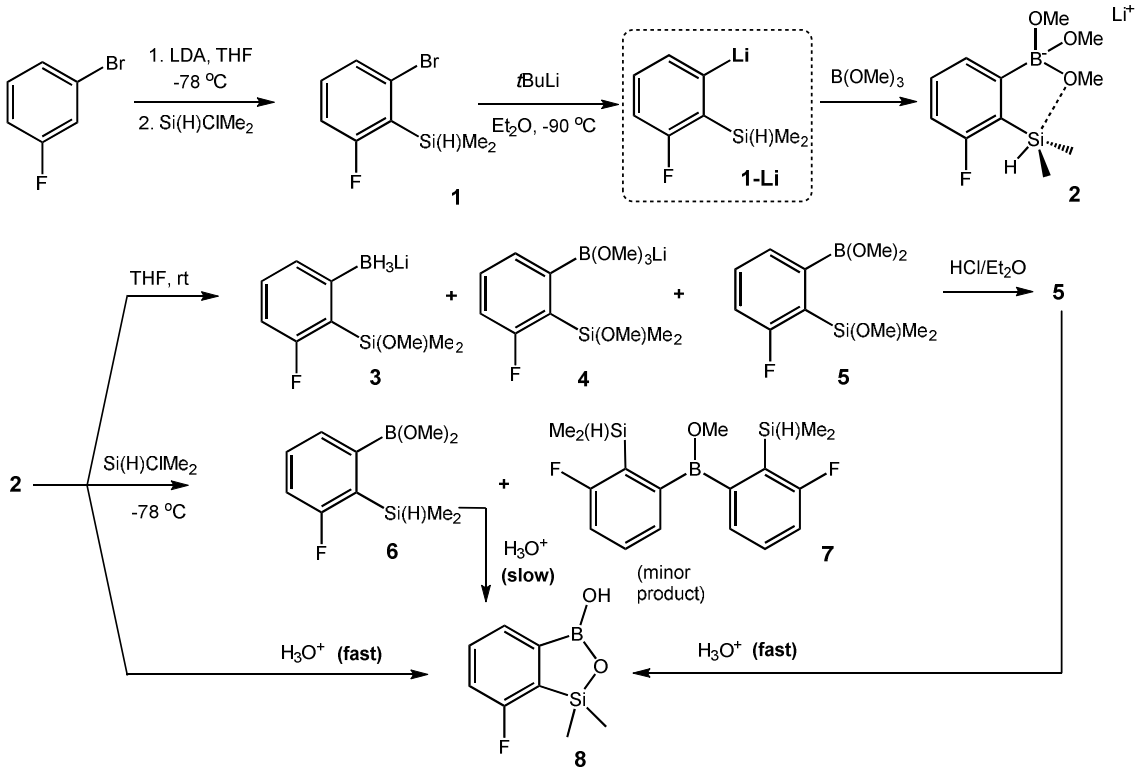

Scheme 2. Formation and transformations of $Si(H)Me_2$-substituted arylboronate ate complex **2**.

View Article Online
DOI: 10.1039/C7DT04858K

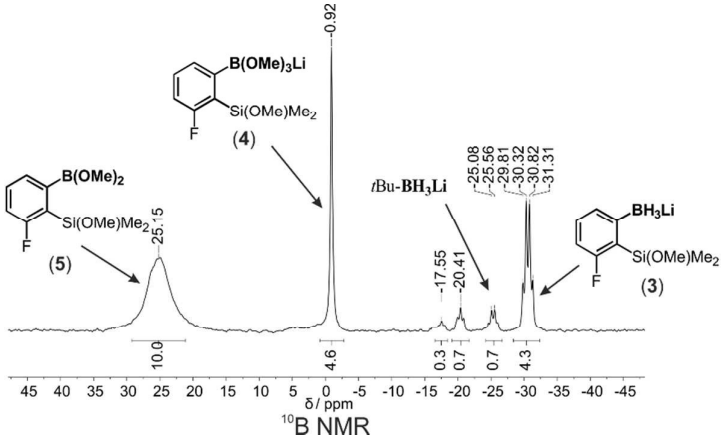

Figure 1. ^{10}B NMR spectrum of a reaction mixture obtained upon treatment of **2** with $B(OMe)_3$.

Further studies revealed that the reaction of **1-Li** with $B(OiPr)_3$ in the ratio of 2:1 followed by hydrolysis gave a borinate-type species **9** as a sole product in good yield (ca. 70%) (**Scheme 3**). The X-ray diffraction analysis revealed that its molecular structure features the spiro arrangement of a central boron atom linking two benzosiloxaborole systems (**Figure 2**). Molecules form centrosymmetric dimers due to strong and symmetrical hydrogen bonds (O…O distance is only 2.432 Å). Notable, the acidity of **9** (pK_a = 3.5 in MeOH/H_2O, 1:1) is strongly enhanced with respect to the related benzosiloxaborole (pK_a = 7.2 ppm). Respective ^{1}H and ^{13}C NMR spectra show broad single resonance of methyl groups, which points to a dynamic character of the molecule at room temperature. According to VT NMR studies (Figure S2, ESI), it seems that the H-bonded dimeric structure of **9** is conformationally stable (on the NMR time scale) at low temperatures in $CDCl_3$. On the other hand, at higher temperatures the Si(OH)-B dative bond dissociates enabling the free rotation around the B-C(aryl) bond, which in turn allows for coordination of Si-OH oxygen atom from an opposite side. Notably, a totally different behavior of **9** is observed in acetone solution. Multinuclear NMR and mass spectral data indicate that most probably it undergoes a slow isomerization (within several hours) to a 8-membered cyclic borinic acid **10** comprising Si–O–Si linkage. The process is reversible as after solvent evaporation the re-formation of single crystals of **9** was confirmed by X-ray diffraction. On the other hand, we have also found that compound **10** undergoes slow degradation in acetone solution after prolonged exposure to air (> 7 d). This behavior is typical for diarylborinic systems. A detailed discussion of observed phenomena is given in the ESI.

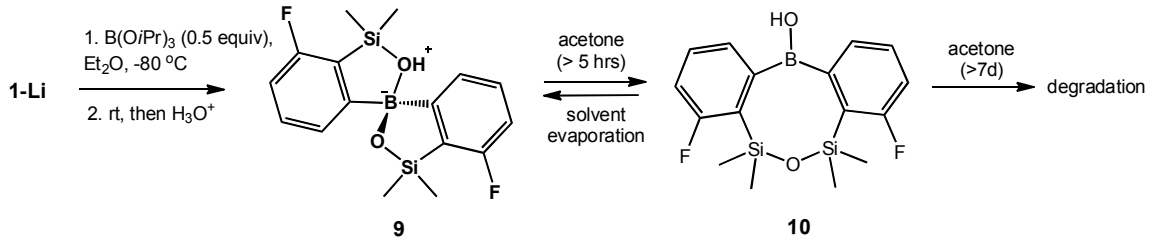

View Article Online
DOI: 10.1039/C7DT04858K

Scheme 3. The synthesis of spiro-bis(siloxa)borinate derivative **9** and its subsequent transformation to siloxane **10**.

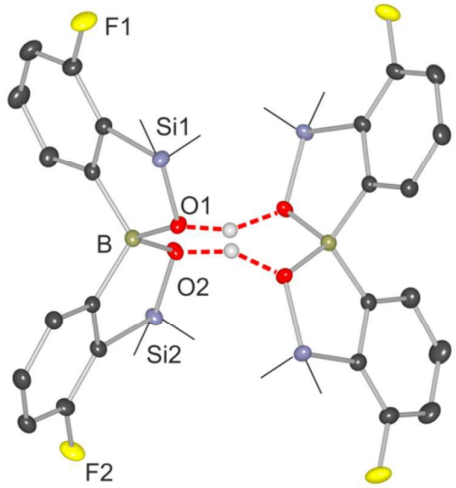

Figure 2. Crystal structure of **9** showing the formation of a dimer with two strong and symmetrical hydrogen-bond O…H…O interactions.

Si–H bond activation with ortho-assisting carbon- and phosphorus-based groups. The discussed above mechanism for the activation of Si–H bond via O…Si coordination should also operate for other *ortho*-assisting groups. Thus, we have carboxylated a suspension of aryllithium **1-Li** in Et_2O with gaseous CO_2 at –90 °C. The mixture was evaporated to dryness under reduced pressure to leave a white solid **11** well soluble in THF. The ^{29}Si HMBC spectrum of the solution in C_6D_6 showed a resonance at –26.0 ppm which points to some additional shielding of silicon atom in $SiHMe_2$ group due to interaction with the carboxylate oxygen atom. Respective ^1H NMR spectrum shows broadened resonances of protons from the $Si(H)Me_2$ group as well as two aromatic protons located *ortho* and *meta* to the carboxylate group. This points to a fluxional behaviour of obtained compound, which can be due to the lability of dative oxygen-silicon interaction. However, it should be stressed that activation of Si–H bond is strong as the addition of water results in vigorous H_2 evolution giving rise to benzosilalactone **12** ($\delta^{29}Si$ = 20.5 ppm, **Scheme 4**). Formation of 5-membered silactone ring was also confirmed by X-ray diffraction analysis (**Figure 3**). In another experiment, **1-Li** was quenched with DMF. Hydrolysis of the adduct afforded 1,3-bis(2-fluoro-6-formylphenyl)-1,1,3,3-tetramethyldisiloxane **14** ($\delta^{29}Si$ = –1.36 ppm, **Scheme 4**) resulting from facile cleavage of the Si–H bond. This suggests that activation of the Si–H bond is achieved through the aminoalkoxide interaction with silicon atom in the intermediate **13**. Hydrolysis leads to cleavage of the Si–H bond followed by subsequent condensation of SiOH fragments to the siloxane bridge (with concomitant liberation of pendant formyl groups).

In the next step we have studied the effect of a phosphorus-based functional group. The reaction of **1-Li** with $(EtO)_2P(O)Cl$ and subsequent hydrolysis resulted in diethyl aryl phosphonate **15** obtained in the initial step as a crude material and identified by ^1H and ^{31}P NMR spectroscopy. This indicates that the phosphonate ester group does not activate the Si–H

View Article Online
DOI: 10.1039/C7DT04858K

bond significantly. However, in the presence of water **15** undergoes slow transformation (within several days) to a novel benzophosphoxasilole heterocycle **16** with concomitant H_2 evolution. We suppose that hydrolysis of one of POEt groups is a rate-limiting step *en route* to **16**. It liberates the anionic *O*-ethyl phosphonate function which is able to activate the Si–H bond effectively via generation of a hypervalent silicon species. Formation of **16** was clearly established by ^{1}H NMR spectrum showing signals of two non-equivalent methyl groups at Si centre. ^{29}Si NMR chemical shift (δ^{29}Si =16.85 ppm) also points to a formation of a 5-membered ring involving the $ArSi(CH_3)_2O$ moiety.[12,13]

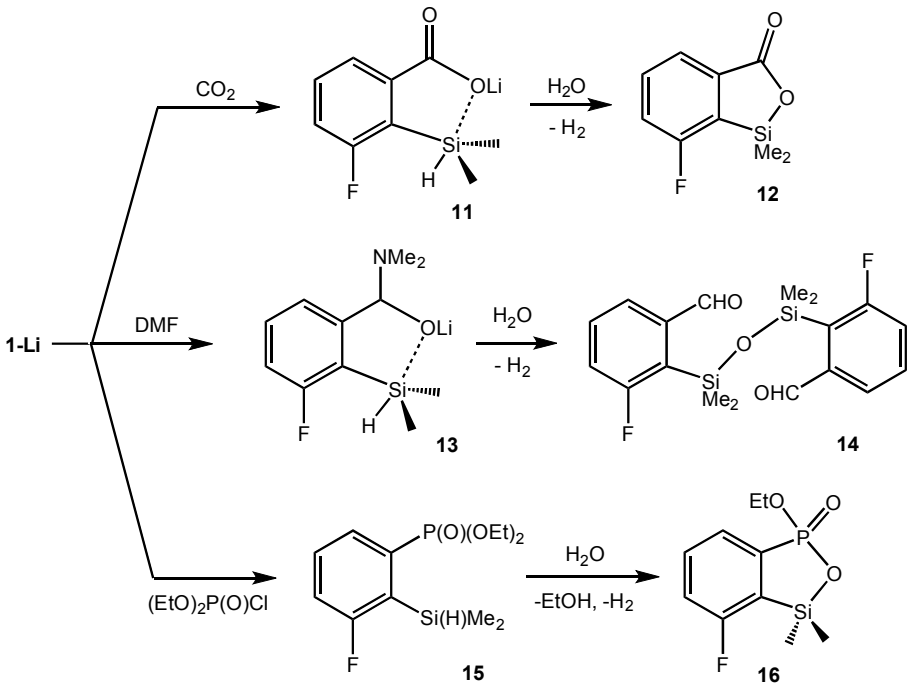

Scheme 4. Si–H bond activation with selected *ortho*-assisting carbon- and phosphorus-based groups.

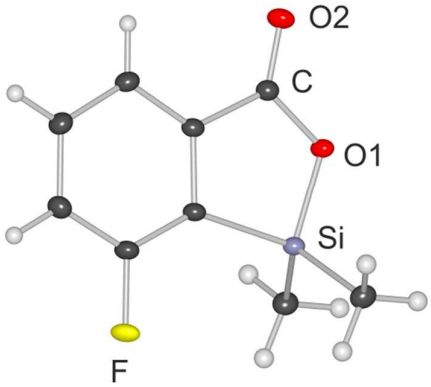

Figure 3. Crystal structure of benzosilalactone **12**.

Interestingly, trapping of **1-Li** with PhCHO gave rise to two silicon-containing compounds with concomitant formation of benzyl alcohol (**Scheme 5**). One can assume that benzosilole **17** is produced via a mechanism similar to that operative for **12**. The formation of

View Article Online
DOI: 10.1039/C7DT04858K

diarylsilane **18** is rather unexpected and can be rationalized in terms of an attack of aryl carbanion on silicon atom in mixed aryllithium/alkoxide aggregate, which can persist during benzaldehyde quench.[20] Presumably, Si–H bond activation in an intermediate five-coordinated silicon species results in hydride transfer to benzaldehyde. The crude reaction mixture contained **17** and **18** in the ratio of 1:2. Both products were separated by column chromatography. The structure of **18** was confirmed by HRMS analysis and multinuclear NMR spectroscopy. Specifically, HMBC $^{1}H,^{29}Si$ NMR spectra showed two signals at –9.59 and –20.52 ppm which can be assigned to Ar_2SiMe_2 and $ArSi(H)Me_2$ moieties, respectively.

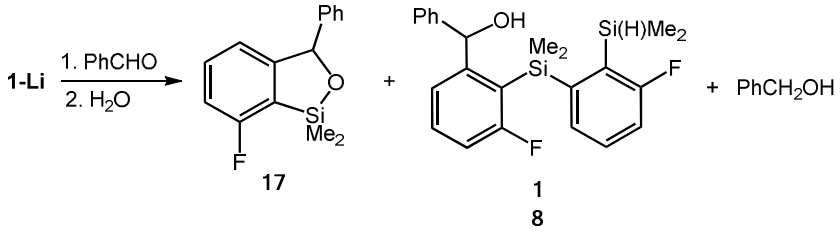

Scheme 5. Reaction of **1-Li** with benzaldehyde.

The observation of the formation of benzyl alcohol is in line with our recent studies on synthesis of formyl-substituted benzosiloxaboroles which showed that reduction of the CHO group can also occur under aqueous acidic conditions required for initial hydrolysis of corresponding acetal precursors.[13] Consequently, the reducing potential of **2** towards various functionalized benzaldehydes was investigated. In all cases, reduction of the formyl group occured resulting in the formation of mixtures containing respective benzyl alcohols and benzosiloxaborole **8** as a by-product (**Scheme 6**, for details, see Supporting Information, **Table S1**). The reaction is chemoselective as other unsaturated functionalities such as CN, COMe, COOEt and NO_2 were inert. One can assume that the hydride transfer occurs directly from the activated hypervalent silicon atom in **2** to the formyl group. This is supported by the fact that the reagent **11** bearing carboxylate group has proved to be also effective reducing agent towards the formyl group of 4-cyanobenzaldehyde.

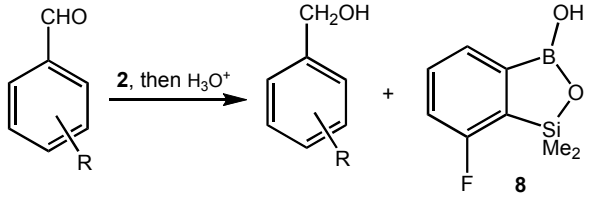

Scheme 6. Reduction of benzaldehydes with the boronic ate complex **2** (details are given in the Supporting Information, **Table S1**).

Further insight into possible activation modes of the Si–H bond in the context of hydrosilylation reaction was provided by the attempted synthesis of cyano-substituted benzosiloxaborole **20** from 3-bromo-2-dimethylsilylbenzonitrile **19**. In our recent study two examples of related cyano-substituted benzosiloxaboroles were obtained in good yields.[13] To

View Article Online
DOI: 10.1039/C7DT04858K

our surprise, a mixture contains mainly formyl-substituted compound **21** resulted from the reduction of cyano group and subsequent hydrolysis of imine (**Scheme 7**). Formation of **21** can be reasonably explained by means of a cooperative mechanism[21] involving coordination of oxygen atom from the boronate group to the silicon centre resulting in a concomitant intramolecular hydride transfer to the electrophilic nitrile carbon atom.

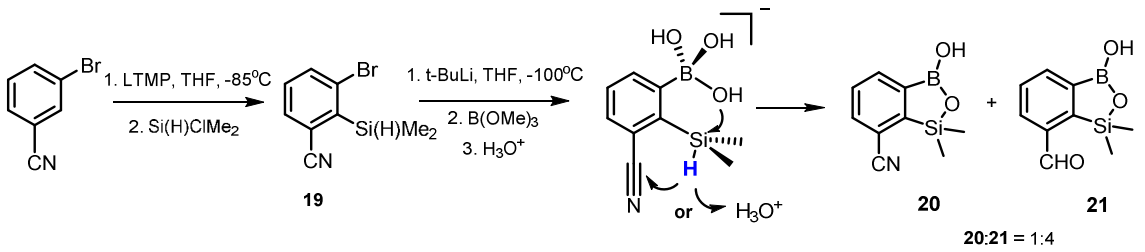

Scheme 7. Reduction of the CN group via boronic-group assisted intramolecular hydrosilylation.

Computational studies on plausible mechanistic pathways.

In order to gain a deeper insight into mechanism of observed Si–H bond activation we have performed a series of DFT (M06-2X[22]/6-31+G(d)[23]) theoretical calculations in *Guassian09*.[24] Our intention was to (i) compare the reactivity of Si–H and Si–C bonds in the five-coordinated silicon intermediates resulted from the inter- or intramolecular reaction with model base, (ii) evaluate the kinetics of Si–H bond activation effected by studied functional groups attached at the *ortho* position, (iii) compare two considered activation modes of boron-containing group (via Si–H…B bridge formation or oxygen-silicon coordination). To simplify calculations, we have used unsubstituted phenyldimethylsilane $PhSi(H)Me_2$ and analogous compounds bearing anionic (CH_2O^-, $CH(NMe_2))O^-$, COO^-, $B(OH)_3^-$) or neutral ($B(OH)_2$, $P(O)(OEt)_2$) functional groups attached at the *ortho* position.

In this work we have clearly demonstrated that the presence of anionic or neutral functional group bearing oxygen atom facilitates activation of Si–H bond in the neighboring $Si(H)Me_2$ group. However, this process may compete with the dissociation of silicon-aryl bond. In a more recognized mechanistic pathway, the reaction of silanes with mild to strong bases such as OH^-, CH_3O^-, NH_2^- involves formation of five-coordinated silicon ate-complex followed by elimination of allyl or aryl substituents.[18,25] Indeed, the reaction of **1** with NaOH (in aqueous or THF solutions) generates phenyl anion which is immediately quenched with water or trapped with benzaldehyde under *in situ* conditions (**Scheme 8**). The latter reaction was observed previously for related arylsilanes using TBAF as a base.[26]

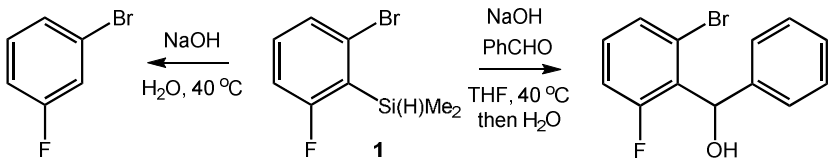

Scheme 8. Testing the reactivity of arylsilane toward OH^-.

View Article Online
DOI: 10.1039/C7DT04858K

To compare the reactivity of Si–H and Si–C bonds we have first optimized the geometry of model hypervalent silicon complexes resulted from the inter- (**A**) and intramolecular (**C**) reaction of arylsilane with base (**Scheme 9**, **Table 1**). As the stability of such hypervalent adducts are affected by electronic features of the substituents we supplemented these studies with corresponding perfluorinated analogues (**B** and **D**). To provide more realistic estimation of dissociation energies the anionic charge of the used molecular species were neutralized by the introduction of lithium cation. Furthermore, calculations were performed using conductor polarizable continuum model with THF as a solvent and the temperature set to 25 ^{o}C. According to our estimations the nucleophilic addition of $MeO^{-}(Li^{+})$ to silicon gives small reaction barrier of 18 kJmol^{-1} (**A**) and 6 kJmol^{-1} (**B**). In an intramolecular version of this reaction, coordination of oxygen atom to silicon centre is exothermic and equals to –22 kJmol^{-1} (**C** and **D**). Subsequent decomposition pathways of five-coordinated silicon ate complexes are different for inter- and intramolecular systems. Nevertheless, in all studied cases cleavage of Si–C(Me) bond is strongly disfavored (ΔG = 70-90 kJmol^{-1}). Comparison of intermolecular reaction modes (**A** and **B**) shows that the cleavage of Si–C(Ar) bond is energetically more advantageous than dissociation of Si–H bond, which is in accordance with our experimental observations. In turn, the elimination of the hydride anion is more favored in the case of intramolecular oxygen coordination for **C**. This can be partially ascribed to trans configuration of oxygen with respect to a hydride ligand. However, fluorination of aromatic ring promotes desilylation, i.e., Si–C(Ar) bond cleavage. Thus, for **D** both processes can operate to a similar extent.

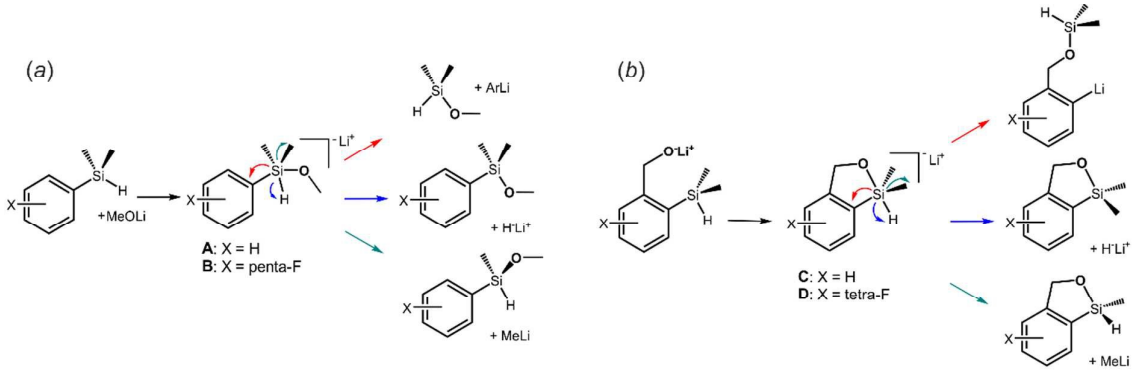

Scheme 9. Possible reaction pathways for the dissociation of five-coordinated silicon ate complexes resulting from the inter- or intramolecular reaction of arylsilane with base.

Table 1. Gibbs free energies (kJmol^{-1}) for the dissociation of five-coordinated silicon ate complexes.

	$Me^{-}Li^{+}$	$Ph^{-}Li^{+}$	$H^{-}Li^{+}$
(**A**) $[PhSi(H)(OMe)Me_2]^{-}Li^{+}$	75	–12	23
(**B**) $[C_6F_5Si(H)(OMe)Me_2]^{-}Li^{+}$	72	–34	12
(**C**) $[Ph(o\text{-}CH_2O)Si(H)Me_2]^{-}Li^{+}$	80	68	15
(**D**) $[C_6F_4(o\text{-}CH_2O)Si(H)Me_2]^{-}Li^{+}$	90	19	21

View Article Online
DOI: 10.1039/C7DT04858K

In the next step we have evaluated the kinetics of *ortho*-assisted activation of Si–H bond via different anionic or neutral functional groups. The Si–H bond cleavage involves hydride ligand transfer from the five-coordinated silicon centre to the electrophile (water). Thus, six-membered cyclic transition state structures have been proposed for observed reactions. The calculations showed that the activation of Si–H bond in simple aryldimethylsilane with water requires a large amount of energy (166 kJmol^{-1}), therefore the process is not observed. Coordination of oxygen atom from a neighbouring functional group to the silicon centre leads to weakening of the Si–H bond and considerably decreases activation barrier (**Table 2**). In the case of anionic $B(OH)_3^-$, $CH(NMe_2)O^-$ (**Figure 4**) groups the activation energy ΔE_a equals to 68 kJmol^{-1} and 88 kJmol^{-1}, respectively, and it drops to only 8 kJmol^{-1} for carboxylate group, while for CH_2O^- group, the coordination of oxygen atom leads to the stable silicon ate complex (–17 kJmol^{-1}). Not surprisingly, for neutral functional groups the kinetics are significantly less favorable ($P(O)(OEt)_2$: ΔE_a = 99 kJmol^{-1}, $B(OH)_2$: ΔE_a = 120 kJmol^{-1}). In all studied cases the Si–H bonds are noticeably elongated in TS (1.58-1.82 Å) with respect to starting compounds (1.49 Å). The previously considered reaction pathway involving the formation of Si–H…B bridge required the coordination of water molecule to the silicon centre and is kinetically unfavorable as the reaction barrier is 122 kJmol^{-1}, which is by 54 kJmol^{-1} higher than the activation through coordination of the $B(OH)_3^-$ oxygen atom to silicon. Nevertheless, it is noticeable that both reaction pathways may compete in neutral boronic compounds such as **6**.

Table 2. Energy barriers for the Si–H bond activation processes in the reaction of 2-R substituted aryldimethylsilane with water or benzaldehyde (values in brackets).

R (neutral)	H	$B(OH)_2$[a]	$B(OH)_2$[b]	$P(O)(OEt)_2$
ΔE / kJmol^{-1}	166 (182)	120	122	99
R (anionic)	$B(OH)_3^-$	CH_2O^- [c]	COO^-	$CH(NMe_2)O^-$
ΔE / kJmol^{-1}	68 (63)	–17	8	88

[a]via coordination of B–O(H)…Si bond, [b]via formation of Si–H…B bridge, [c]located as minimum on potential energy surface.

View Article Online
DOI: 10.1039/C7DT04858K

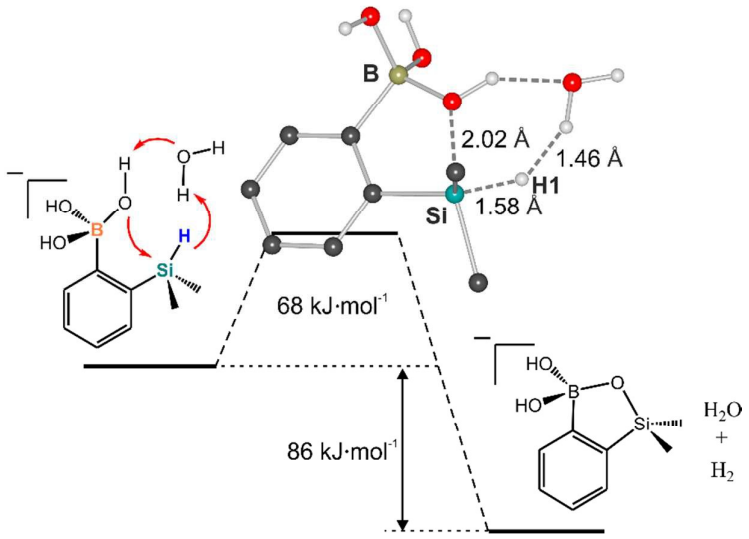

Figure 4. The reaction pathway for activation of Si–H bond by boronate group in the presence of water. Reaction pathways for other tested systems are presented in Supporting Information.

Considering the hydrosilylation of benzaldehyde, the reduction with boronated arylsilane is again kinetically favored over the reduction with simple $PhSi(H)Me_2$ (63 $kJmol^{-1}$ vs. 182 $kJmol^{-1}$). Furthermore, the obtained energy barriers are slightly lower when compared to corresponding processes with water, however, the latter process may still occur to some extent. In the specific case of cyano-substituted compound **19**, reduction apparently involves an intramolecular hydride transfer from five-coordinated silicon center to the adjacent electrophilic carbon atom. According to DFT calculations the reaction barrier is 82 $kJmol^{-1}$, which is by 14 $kJmol^{-1}$ higher than dehydrogenation with water. However, since the reduction of CN group is additionally favored (due to its intramolecular character), both reactions can be observed experimentally.

Conclusions

In our previous work we proposed that the activation of the Si–H bond by adjacent $B(OH)_2$ can be explained assuming the transition state featuring Si–H…B bridge in accordance with a mechanism observed for other (and generally stronger) boron Lewis acids. However, a closer inspection revealed that the process is driven by a coordination of an oxygen atom from the $B(OH)_2$, or more probable – the anionic $B(OH)_3^-$ group (ΔE = 63 $kJmol^{-1}$), to the silicon atom. This results in a facile release of a hydridic ligand which in the absence of an external electrophile is transferred to the boron atom resulting in formation of the $ArBH_3^-$ anion as one of final products. The activation of two Si–H bonds in a respective diarylborinic system gives rise to an unprecedented spiro-bis(siloxa)borinate derivative which is a relatively strong Brønsted acid and shows dynamic behavior in solution. The activating effect of other related functional group bearing an anionic or neutral oxygen atom such as COO^- and $P(O)(OEt)_2$ was also observed. The products of these reactions were respective benzoxasiloles including heterocycles featuring Si–O–C(O) or Si–O–P linkage. The activation effect was also observed in the case of $CH(NMe_2)O^-$ and $CH(Ph)O^-$ groups, however, acyclic compounds **14** and **18**,

View Article Online
DOI: 10.1039/C7DT04858K

were obtained as main products. The activated Si–H bond is also able to reduce various benzaldehydes. Finally, theoretical calculations indicate that the intramolecular coordination of silicon atom effectively prevents the cleavage of Si-aryl bond. In contrast, this process is favored in the case of an intermolecular reaction when arylsilane of the type $ArSi(H)Me_2$ is attacked by an external oxygen nucleophile such as MeO^-. Finally, calculated reaction barriers for tested arylsilanes strongly depend on charge and nucleophilicity of ortho-assisting functional group.

Experimental Section

General comments. Solvents used for reactions were dried by refluxing with sodium/benzophenone and distilled under argon. Starting materials including various benzene derivatives, $Si(H)ClMe_2$, $B(OMe)_3$ were used as received without further purification. NMR spectra were recorded on 300 MHz (Bruker Avance-III, nucleus: ^1H, ^{11}B, ^{13}C, ^{19}F), 400 MHz (Agilent, nucleus: ^1H, ^{13}C, ^{19}F) and 500 MHz (Agilent, nucleus: ^1H, ^{10}B, ^{29}Si) spectrometers. In the ^{13}C NMR spectra the resonances of boron-bound carbon atoms were not observed in most cases because of their broadening by a quadrupolar boron nucleus. ^1H, ^{13}C and ^{29}Si NMR chemical shifts are given relative to TMS. ^{10}B, ^{11}B and ^{19}F NMR chemical shifts are given relative to $BF_3{\cdot}Et_2O$ and $CFCl_3$, respectively.

Synthesis:

Spiro-bis(siloxa)borinate 9. A solution of 1-bromo-3-fluoro-2-dimethylsilylbenzene **1** (2.33 g, 10 mmol) in Et_2O (10 mL) was added dropwise to a solution of *t*-BuLi (1.7 M in pentane, 12 mL, 20 mmol) in Et_2O (30 mL) at –90 °C. A mixture was stirred for 20 min at –90 °C and the obtained white suspension of **1-Li** was treated with $B(O\textit{i}Pr)_3$ (1.15 mL, 5 mmol). The mixture was allowed to warm slowly to the ambient temperature with stirring and quenched with 1 M aq. H_2SO_4. Hydrogen evolution was observed immediately. The aqueous phase was separated followed by the extraction with Et_2O (2 × 20 mL). The extracts were added to the organic phase, which was dried with anhydrous $MgSO_4$, filtered and concentrated under reduced pressure. Solvents were removed to leave a white waxy residue which was stirred overnight with hexane (10 mL). The resulting suspension was filtered and the crude product was crystallized from $CHCl_3$/hexane (1:1) to give **8** as colorless crystals, m.p. 173-175 °C. Yield: 1.2 g (69%). ^1H NMR (400 MHz, $CDCl_3$) δ 7.33-7.23 (m, 2H), 6.94–6.79 (m, 4H), 0.29 (broad, 12H) ppm. ^1H NMR (300 MHz, Acetone-d_6) δ 7.32 (ddd, J = 8.1, 7.2, 5.7 Hz, 2H), 6.96-6.87 (m, 4H), 0.48 (s, 12H) ppm. ^1H NMR (300 MHz, D_2O/DMSO/K_2CO_3) δ 7.07 (ddd, J = 8.0, 7.1, 5.8 Hz, 2H), 6.77–6.61 (m, 4H), 0.36 (s, 6H), 0.32 (s, 6H) ppm. ^{13}C NMR (101 MHz, $CDCl_3$) δ 165.05 (d, J = 244.3 Hz), 160.95, 132.57 (d, J = 6.3 Hz), 125.44 (d, J = 2.7 Hz), 124.51 (d, J = 28.7 Hz), 112.53 (d, J = 23.7 Hz), 0.38 (broad) ppm. ^{11}B NMR (96 MHz, $CDCl_3$) δ 12.6 ppm. ^{11}B NMR (96 MHz, Acetone-d_6) δ 17.6 ppm. ^{11}B NMR (96 MHz, D_2O/DMSO/K_2CO_3) δ 8.4 ppm. ^{19}F NMR (376 MHz, $CDCl_3$) δ –104.16 (ddd, J = 8.0, 5.7, 2.5 Hz) ppm. ^{19}F NMR (282 MHz, Acetone-d_6) δ –105.96 (ddd, J = 8.1, 5.7, 2.6 Hz) ppm. ^{29}Si NMR (99 MHz, $CDCl_3$) δ 24.40 ppm. ^{29}Si NMR (99 MHz, D_2O/DMSO/K_2CO_3) δ 12.90 (d, J = 2.3 Hz) ppm. HRMS (EI): calcd. for $C_{16}H_{19}BF_2O_2Si_2$ $[M\text{-}CH_3]^+$ 333.0750 found 333.0758.

View Article Online
DOI: 10.1039/C7DT04858K

Silalactone (12). The suspension of **1-Li** was obtained as described above. It was cooled to –100 °C with vigorous stirring and carboxylated by saturation with dried gaseous CO_2. The resulting white suspension was warmed slowly to the room temperature and was quenched with 2 M aq. H_2SO_4 to reach the pH = 1-2. The aqueous phase was separated followed by the extraction with Et_2O (2 × 20 mL). The extracts were added to the organic phase, which was dried with anhydrous $MgSO_4$ and concentrated under reduced pressure. A viscous oily residue was dissolved in hexane (5 mL) and cooling to –30 °C gave the product **12** as colorless crystals, m.p. 64-66 °C. Yield: 0.40 g (83%). ^{1}H NMR (400 MHz, $CDCl_3$) δ 7.89 (ddd, *J* = 7.5, 1.4, 0.7 Hz, 1H), 7.63 (ddd, *J* = 8.1, 7.5, 5.4 Hz, 1H), 7.30 (ddd, *J* = 8.1, 6.8, 0.7 Hz, 1H), 0.64 (s, 6H) ppm. ^{13}C NMR (101 MHz, $CDCl_3$) δ 166.84 (d, *J* = 1.5 Hz), 164.45 (d, *J* = 247.6 Hz), 139.36 (d, *J* = 10.0 Hz), 134.18 (d, *J* = 6.9 Hz), 126.76 (d, *J* = 35.1 Hz), 123.72 (d, *J* = 3.3 Hz), 119.93 (d, *J* = 24.0 Hz), –1.52 ppm. ^{19}F NMR (376 MHz, $CDCl_3$) δ –101.80 - –101.88 (m) ppm. ^{29}Si NMR (99 MHz, $CDCl_3$) δ 20.59 ppm. HRMS (EI): calcd. for $C_9H_9FO_2Si$ $[M]^+$ 196.0356; found 196.0352.

1,1'-Bis(2-fluoro-6-formylphenyl)tetramethyldisiloxane (14)

^{1}H NMR (400 MHz, $CDCl_3$) δ 10.31 (s, 1H), 7.72 (d, *J* = 7.5 Hz, 1H), 7.50 (td, *J* = 7.8, 5.4 Hz, 2H), 7.19 (t, *J* = 8.7 Hz, 1H), 0.50 (d, *J* = 2.6 Hz, 8H) ppm. ^{13}C NMR (75 MHz, $CDCl_3$) δ 192.54 (d, *J* = 2.7 Hz), 167.07 (d, *J* = 244.4 Hz), 143.59 (d, *J* = 8.7 Hz), 131.78 (d, *J* = 9.3 Hz), 126.81 (d, *J* = 26.9 Hz), 126.03 (d, *J* = 2.6 Hz), 120.69 (d, *J* = 28.6 Hz), 3.43 (d, *J* = 4.3 Hz) ppm. ^{29}Si{^{1}H} NMR (99 MHz, $CDCl_3$) δ –1.36 ppm. HRMS (EI): calcd. for $C_{18}H_{20}F_2O_3Si_2$ $[M\text{-}CH_3]^+$ 363.0684 found 363.0695.

4-Fluoro-(*P*-ethoxy)(*P*-oxo)benzophosphoxasilole (16)

To a suspension of **1-Li** (5 mmol), $P(O)(OEt)_2Cl$ (0.75 mL, 5 mmol) dissolved in 5 mL Et_2O was added dropwise at –95 °C. The resulting solution was warmed to 0 °C and hydrolyzed with 1.5 M H_2SO_4 to reach pH 2. Then the resulting mixture was warmed to 30 °C and stirred for 24 h. The aqueous phase was separated followed by the extraction with Et_2O (2 × 10 mL). The combined organic phases were washed with 0.01 M NaOH and brine. The organic phase was dried with anhydrous $MgSO_4$ and concentrated under reduced pressure giving the final product as viscous oil (1.10 g, 84%). ^{1}H NMR (400 MHz, $CDCl_3$) δ 7.76-7.40 (m, 2H, Ar), 7.20 (t, *J* = 7.6 Hz, 1H, Ar), 4.10-4.00 (m, 2H, OEt), 1.33 (t, *J* = 7.1 Hz, 3H, OEt), 0.61 (s, 3H, SiMe), 0.58 (s, 3H, SiMe) ppm. ^{13}C NMR (101 MHz, $CDCl_3$) δ 164.70 (dd, *J* = 247.3, 25.3 Hz), 138.98 (dd, *J* = 181.6, 8.7 Hz), 134.26 (dd, *J* = 17.1, 6.9 Hz), 127.84 (dd, *J* = 34.6, 28.5 Hz), 124.83 (dd, *J* = 13.3, 3.4 Hz), 118.45 (dd, *J* = 23.5, 3.1 Hz), 62.79 (d, *J* = 6.2 Hz), 16.40 (d, *J* = 6.3 Hz), –0.52 (d, *J* = 2.8 Hz), –0.68 (d, *J* = 2.8 Hz) ppm. ^{19}F NMR (376 MHz, $CDCl_3$) δ –101.95 - –102.17 (m) ppm.^{31}P{^{1}H} NMR (162 MHz, $CDCl_3$) δ 20.80 (d, *J* = 4.5 Hz) ppm. ^{29}Si{^{1}H} NMR (99 MHz, $CDCl_3$) δ 16.85 (dd, *J* = 7.8, 4.0 Hz) ppm. HRMS (EI): calcd. for $C_{10}H_{14}FO_3PS$ $[M]^+$ 260.0434, found 260.0430.

1,1-Dimethyl-7-fluoro-3-phenylbenzoxasilole (17) and [2-(dimethylsilyl)-3-fluorophenyl][2-(phenylhydroxymethyl)-6-fluorophenyl]dimethylsilane (18). The suspension of **1-Li** (10 mmol scale) was obtained as described above. It was treated with a solution of PhCHO (2.12 g, 20 mmol) in Et_2O (10 mL) at –90 °C. A resulting white suspension was warmed slowly to 0 °C and quenched with 2 M aq. H_2SO_4 to reach the pH =

View Article Online
DOI: 10.1039/C7DT04858K

1-2. The aqueous phase was separated followed by the extraction with Et_2O (2 × 20 mL). The extracts were added to the organic phase, which was dried with anhydrous $MgSO_4$ and concentrated under reduced pressure. According to 1H NMR, the proportion of **17**:**18** is 1:2. A viscous oily residue was subjected to column chromatography (silica gel, eluent hexane/EtOAc, 20:1) to give **17** as a white solid and **18** as a colorless viscous oil. The fraction of benzyl alcohol was also isolated.

Compound **17**: m.p. 56-57 °C, 0.43 g. ^{1}H NMR (300 MHz, $CDCl_3$) δ 7.49-7.17 (m, 6H), 6.99-6.89 (m, 1H), 6.88-6.80 (m, 1H), 6.18 (s, 1H, CH), 0.62 (s, 3H, Me), 0.54 (s, 3H, Me) ppm. ^{19}F NMR (282 MHz, $CDCl_3$) δ –102.19 - –102.24 (m) ppm. ^{13}C NMR (75 MHz, $CDCl_3$) δ 164.9 (d, *J* = 244.1 Hz), 155.6 (d, *J* = 10.2 Hz), 143.2 , 132.7 (d, *J* = 7.1 Hz), 128.6, 128.0, 127.1, 121.7 (d, *J* = 36.8 Hz), 119.8 (d, *J* = 3.2 Hz), 113.1 (d, *J* = 24.2 Hz), 84.0 , 1.2 , 0.4 ppm. ^{29}Si NMR (99 MHz, $CDCl_3$) δ 27.24 ppm. HRMS (EI): calcd. for $C_{15}H_{15}FOSi$ $[M]^+$ 258.0876; found 258.0869.

Compound **18**: 0.76 g. ^{1}H NMR (500 MHz, $CDCl_3$) δ 7.52 (dt, *J* = 7.3, 1.2 Hz, 1H), 7.41 (ddd, *J* = 8.2, 7.3, 6.0 Hz, 1H), 7.35-7.18 (m, 4H), 7.10-7.01 (m, 3H), 6.98 (dd, *J* = 7.8, 1.0 Hz, 1H), 6.93 (ddd, *J* = 9.5, 8.1, 1.0 Hz, 1H), 5.87 (d, *J* = 3.1 Hz, 1H, CH), 4.60-4.50 (m, 1H, SiH), 1.66 (d, *J* = 3.7 Hz, 1H, OH), 0.77 (d, *J* = 3.5 Hz, 3H, Ar_2SiMe_2), 0.70 (d, *J* = 2.2 Hz, 3H, Ar_2SiMe_2), 0.15 (ddd, *J* = 11.6, 3.8, 1.9 Hz, 6H, $Si(H)Me_2$) ppm. ^{13}C NMR (75 MHz, $CDCl_3$) δ 168.42 (d, *J* = 241.4 Hz), 166.94 (d, *J* = 242.0 Hz), 151.22 (d, *J* = 8.4 Hz), 149.52 (dd, *J* = 6.7, 1.5 Hz), 143.20 , 131.75 (d, *J* = 9.7 Hz), 131.51 (d, *J* = 8.2 Hz), 130.10 (d, *J* = 2.5 Hz), 129.69 (d, *J* = 26.8 Hz), 128.19 , 127.26 , 126.50 , 124.74 (d, *J* = 26.0 Hz), 124.47 (d, *J* = 2.7 Hz), 115.90 (d, *J* = 26.3 Hz), 114.54 (d, *J* = 27.6 Hz), 73.30 (d, *J* = 2.1 Hz), 2.55 (d, *J* = 5.3 Hz), 2.51 (d, *J* = 5.5 Hz) –3.71 (dd, *J* = 9.1, 3.5 Hz) ppm. ^{19}F NMR (282 MHz, $CDCl_3$) δ –93.29 - –95.73 (m), –97.17 - –98.27 (m) ppm. ^{29}Si HMBC NMR (99.3 MHz, $CDCl_3$) δ –9.59, –20.52 ppm. HRMS (ESI): calcd. for $C_{23}H_{26}F_2OSi_2$ $[M+Na]^+$ 435.1388; found 435.1377.

3-Bromo-2-(dimethylsilyl)benzonitrile (**17**): A solution of 3-bromobenzonitrile (18.2 g, 0.1 mol) in THF (80 mL) was added at –100 °C to a stirred solution of LDA, freshly prepared from diisopropylamine (10.5 g, 0.105 mol) and *n*BuLi (10 M, 10 mL, 0.1 mol) in THF (150 mL). After ca. 30 min stirring at ca. –95 °C chlorodimethylsilane (10.0 g, 0.106 mol) was added slowly. The mixture was stirred for 30 min at –85 °C and then allowed to warm to the room temperature. Solvents were removed under reduced pressure and the residue was redissolved in hexane (100 mL). The mixture was filtered under argon through a Celite pad to remove LiCl byproduct. The filtrate was concentrated and the residue was subjected to a fractional distillation under reduced pressure. The product was obtained as a colorless liquid, b.p. 84-87 °C (1 Tr). Yield 20.7 g (86%). ^{1}H NMR (400 MHz, $CDCl_3$) δ 7.74 (dd, *J* = 8.1, 1.1 Hz, 1H), 7.65 (dd, *J* = 7.7, 1.1 Hz, 1H), 7.30 (t, *J* = 7.9 Hz, 1H), 5.03 (sp, *J* = 3.9 Hz, 1H), 0.55 (d, *J* = 3.9 Hz, 6H) ppm. ^{13}C NMR (100.6 MHz, $CDCl_3$) δ 142.51, 136.94, 132.90, 131.38, 130.91, 120.39, 118.34, –3.44 ppm. Anal. Calcd for $C_9H_{10}BrNSi$ (240.17): C, 45.01; H, 4.20. Found: C, 44.95; H, 4.54.

7-Cyano-1,3-dihydro-3-hydroxy-1,1-dimethyl-1,2,3-benzosiloxaborole (18) and 7-formyl-1,3-dihydro-3-hydroxy-1,1-dimethyl-1,2,3-benzosiloxaborole (19): Compound **17** (2.40 g,

View Article Online
DOI: 10.1039/C7DT04858K

0.01mol) in 5 mL of THF was slowly added to a stirred solution of *t*-BuLi (1.7 M, 12.0 ml, 0.02 mol) in THF/Et_2O (15/15 mL) at –75 ^oC. After 1 h of stirring a solution of $B(OEt)_3$ (3.4 mL, 0.02 mol) in 5 mL of THF was added dropwise. After 0.5 h of stirring the solution was warmed to –15 ^oC and hydrolyzed with 1.5 M H_2SO_4 to pH = 3-4. The water phase was separated followed by extraction with Et_2O (20 mL). Organic phases were combined, dried with anhydrous $MgSO_4$ and concentrated under reduced pressure. The precipitate was dissolved in hexane, then water was added and the mixture was heated to 60 ^oC. The hexane phase was separated and cooled to –20 ^oC, which resulted in product crystallization. It was filtered and dried under reduced pressure to give the mixture of **18** and **19** in the ratio of 1:4. Due to a similar character of obtained compounds their attempted separation failed. ^1H NMR (300 MHz, $CDCl_3$): **17**: δ 8.03 (dd, *J* = 7.4, 1.0 Hz, 1H, Ph), 7.77 (dd, *J* = 7.7, 1.0 Hz, 1H, Ph), 7.58 (t, 1H, *J* = 7.6, Ph), 5.62 (s, 1H, OH), 0.58 (s, 6H, $SiMe_2$); **18**: 10.06 (s, 1H, CHO), 8.09 (dd, *J* = 7.3, 1.0 Hz, 1H, Ph), 7.94 (dd, *J* = 7.5, 1.1 Hz, 1H, Ph), 7.69 (t, *J* = 7.4 Hz, 1H, Ph), 5.71 (s, 1H, OH), 0.51 (s, 6H, $SiMe_2$) ppm.

Testing the reactivity of 1 with NaOH. (a) Reaction in water. A solution of compound **1** (0.23 g, 1mmol) in 3 mL of THF was added to the 10 mL of 5% $NaOH_{aq}$. The reaction was stirred at 40 ^oC for 1h. The evolution of hydrogen gas was observed. The reaction was extracted with Et_2O (5 mL) and organic phase was concentrated in vacuo. The GC-MS analysis showed complete desilylation of **1** to give 1-bromo-3-fluorobenzene; (b) Reaction in THF. A solution of **1** (0.23 g, 1 mmol) was mixed with benzaldehyde (0.106 g, 1 mmol) in THF and a saturated solution of NaOH (0.040 g, 1 mmol) in THF was added. The reaction was stirred at 40 ^oC for 1 h. The organic phase was washed with brine and concentrated in vacuo. The GC-MS analysis show the formation of (2-bromo-6-fluorophenyl)(phenyl)-methanol (88% conversion with respect to **1**) along with 1-bromo-3-fluorobenzene (12% with respect to **1**), benzyl alcohol (6% conversion with respect to PhCHO), and benzoic acid (6% conversion with respect to PhCHO), two latter products presumably resulting from Cannizzaro reaction of PhCHO.

Structural measurement and refinement details. The single crystals of **9** and **12** were measured at 100 K on SuperNova diffractometer equipped with Atlas detector (Cu-K_α radiation, λ = 1.54184 Å). Data reduction and analysis were carried out with the CrysAlisPro program.[27] All structures were solved by direct methods using SHELXS-97[28] and refined using SHELXL-2014.[29] All non-hydrogen atoms were refined anisotropically. Crystallographic Information Files (CIFs) have been deposited with the Cambridge Crystallographic Data Centre as supplementary publications no. 1581785 (**9**) and 1581784 (**12**).

Crystal data for **9**: $C_{16}H_{19}BF_2O_2Si_2$, M_r = 348.30 a.u.; monoclinic; *C* 2/*c*; *a* = 20.3719 (4) Å, *b* = 8.5430 (2) Å, *c* = 20.6238 (5) Å, β = 90.992 (2)°, *V* = 3588.77 (14) $Å^3$; d_{calc} = 1.289 $g{\cdot}cm^{-3}$; μ = 0.221 mm^{-1}; *Z* = 8; F(000) = 1456; number of collected / unique reflection (R_{int} = 2.25%) = 24087 / 6060, R[F] / wR[F] (I ≥ 3σ(I)) = 3.45 % / 10.15%, $\Delta\varrho_{res}^{(min/max)}$ = −0.51/ +0.47 $e{\cdot}Å^{-3}$.

Crystal data for **12**: $C_9H_9FO_2Si$, M_r = 196.25 a.u.; monoclinic; *C* 2/*m*; *a* = 17.2067 (7) Å, *b* = 7.1378 (3) Å, *c* = 7.5388 (3) Å, β = 100.265 (4)°, *V* = 911.08 (7) $Å^3$; d_{calc} = 1.431 $g{\cdot}cm^{-3}$; μ =

View Article Online
DOI: 10.1039/C7DT04858K

0.235 mm^{-1}; Z = 4; F(000) = 408; number of collected / unique reflection (R_{int} = 3.41%) = 10042 / 1797, R[F] / wR[F] (I ≥ 3σ(I)) = 3.61 % / 11.16%, $\Delta\varrho_{res}^{(min/max)}$ = −0.33/ +0.58 e·$Å^{-3}$.

Computational methods. All geometry optimizations and frequency calculations were carried out with the *GAUSSIAN09*[24] suite of programs and M06-2X[22] functional with 6-31+G(d)[23] was applied to calculate the optimal geometries. The minima were confirmed by vibrational frequency calculations [M06-2X/6-31+G(d)] within harmonic approximation (no imaginary frequencies). To optimize the structures of transition states, a synchronous transit-guided quasi-Newton approach (QST3) was applied. In this method, three input structures are needed: one corresponds to reactants, one to products and one is a guess of a transition state. To verify the structures of the transition states, frequency calculations were carried out at the same level of theory. One imaginary frequency was found in all cases except of CH2O-functional group, where corresponding state bearing five-coordinated silicon centre was located as minimum on potential energy surface. As all reductions processes proceed in THF, the computations were performed using reaction field calculation with the integral equation formalism model [SCRF(CPCM, solvent = THF)].[30] The geometry of optimized structures and transition states are provided in Supporting Information. Gibbs free energies were obtained from the frequency calculations with the temperature set to 298 K.

Acknowledgment

This work was supported by Warsaw University of Technology. K. Durka thanks the Foundation for Polish Science for financial support within the START program. The X-ray measurements were undertaken in the Crystallographic Unit of the Physical Chemistry Laboratory at the Chemistry Department of the University of Warsaw. Authors thank Prof. Krzysztof Woźniak for providing the access to this laboratory. We would like to thank Jacek Olędzki from Institute of Biochemistry and Biophysics Polish Academy of Sciences for performing MS analysis and Marcin Wilczek from Faculty of Chemistry, University of Warsaw, for performing gaseous 1H NMR experiment. Authors thank the Interdisciplinary Centre for Mathematical and Computational Modelling in Warsaw (G33-14) for providing computational facilities.

References

1. (a) J. Y. Corey, *Chem. Rev.*, 2016, **116**, 11291–11435; (b) J. Y. Corey, *Chem. Rev.*, 2011, **111**, 863–1071; (c) M. C. Lipke, A. L. Liberman-Martin and T. D. Tilley, *Angew. Chem. Int. Ed.* 2017, **56**, 2260–2294; (d) M. Oestreich, J. Hermeke and J. Mohr, *Chem. Soc. Rev*. 2015, **44**, 2202–2220.

2. (a) B. Marciniec*, Hydrosilylation: A Comprehensive Review on Recent Advances, Advances in Silicon Science*, vol. 1, Springer, Germany, 2009, DOI: 10.1007/978-1-4020-8172-9; (b) D. Troegel and J. Stohrer, *Coord. Chem. Rev.*, 2011, **255**, 1440–1459; (c) A. K. Roy, *Adv. Organomet. Chem.*, 2007, **55**, 1–59; (d) E. Plueddemann, *Silane Coupling Agents*, 2nd ed., Plenum Press, New York, 1991; (e) A. F. Noels and A. J. Hubert, *Industrial Applications of Homogeneous Catalysis* (Ed. A. Mortreux), Kluwer, Amsterdam, The Netherlands, 1985, pp. 80–91.

View Article Online
DOI: 10.1039/C7DT04858K

3. (a) H. Nishiyama, H. Sakaguchi, T. Nakamura, M. Horihata, M. Kondo and K. Itoh, *Organometallics*, 1989, **8**, 846–848; (b) B. Tao and G. C. Fu, *Angew. Chem. Int. Ed.*, 2002, **41**, 3892–3894. (c) L. H. Gade, V. Cesar and S. Bellemin-Laponnaz, *Angew. Chem. Int. Ed.* 2004, **43**, 1014–1017; (d) Y. Nishibayashi, I. Takei, S. Uemura and M. Hidai, *Organometallics*, 1998, **17**, 3420–3422; (e) A. R. Chianese and R. H. Crabtree, *Organometallics*, 2005, **24**, 4432–4436; (f) J. Yun and S. L. Buchwald, *J. Am. Chem. Soc.,* 1999, **121**, 5640–5644; (g) B. H. Lipshutz, K. Noson, W. Chrisman, and A. Lower, *J. Am. Chem. Soc.,* 2003, **125**, 8779–8789; (h) H. Mimoun, J. Y. D. S. Laumer, L. Giannini, R. Scopelliti and C. Floriani, *J. Am. Chem. Soc.,* 1999, **121**, 6158–6166; (i) S. Das, D. Addis, S. Zhou, K. Junge and M. Beller, *J. Am. Chem. Soc.,* 2010, **132**, 1770–1771; (j) L. Postigo and B. Royo, *Adv. Synth. Catal.* 2012, **354**, 2613–2618. (k) X. Verdaguer, U. E. W. Lange, M. T. Reding and S. L. Buchwald, *J. Am. Chem. Soc.* 1996, **118**, 6784–6785; (l) H. Gruber-Woelfler and J. G. Khinast, *Organometallics,* 2009, **28**, 2546–2553; (m) B. H. Lipshutz and H. Shimizu, *Angew. Chem. Int. Ed.,* 2004, **43**, 2228–2230; (n) K. A. Nolin, R. W. Ahn and F. D. Toste, *J. Am. Chem. Soc.,* 2005, **127**, 12462–12463; (o) K. A. Nolin, R. W. Ahn, Y. Kobayashi, J. J. Kennedy-Smith and F. D. Toste, *Chem. Eur. J.,* 2010, **16**, 9555–9562. (p) S. Das, B. Wendt, K. Möller, K. Junge and M.Beller, *Angew. Chem. Int. Ed.*, 2012, **51**, 1662–1666; (q) S. Laval, W. Dayoub, A. Favre-Reguillon, M. Berthod, P. Demonchaux, G. Mignani and M. Lemaire, *Tetrahedron Lett.*, 2009, **50**, 7005–7007; (r) D. Addis, S. Das, K. Junge and M. Beller, *Angew. Chem. Int. Ed.,* 2011, **50**, 6004–6011; (s) T. Murai, T. Sakane and S. Kato, *J. Org. Chem.,* 1990, **55**, 449–453; (t) C. Bornschein, S. Werkmeister, K. Junge and M. Beller, *New J. Chem.* 2013, **37**, 2061–2065; (u) D. V. Gutsulyak and G. I. Nikonov, *Angew. Chem. Int. Ed.,* 2010, **49**, 7553–7556; (w) S. Laval, W. Dayoub, L. Pehlivan, E. Métay, D. Delbrayelle, G. Mignani and M. Lemaire, *Tetrahedron Lett.* 2014, **55**, 23–26; (x) S. Laval, W. Dayoub, L. Pehlivan, E. Métay, A. Favre-Reguillona, D. Delbrayelle, G. Mignani and M. Lemaire, *Tetrahedron* 2014, **70**, 975–983.

4. (a) N. Lawrence and S. M. Bushell, *Tetrahedron Lett.,* 2000, **41**, 4507–4512; (b) J. Koller and R. G. Bergman, *Organometallics*, 2012, **31**, 2530–2533.

5. (a) K. Revunova and G. I. Nikono, *Dalton Trans.,* 2015, **44**, 840-866; (b) Y. Izumi, N. Yusuke, H. Nanami, K. Higuichi and M. Ohaka, *Tetrahedron Lett.,* 1991, **32**, 4741–4744; (c) S. Fukuzumi and M. Fujita, *Chem. Lett.,* 1991, 2059–2062; (d) N. Asao, T. Ohishi, K. Sato and Y. Yamamoto, *J. Am. Chem. Soc.,* 2001, **123**, 6931–6932; (e) N. Asao, T. Ohishi, K. Sato and Y. Yamamoto, *Tetrahedron*, 2002, **58**, 8195–8203; (f) M. Hojo, A. Fuji, C. Murakami, H. Aihora, and A. Hosomi, *Tetrahedron Lett.,* 1995, **36**, 571–574; (g) M. Hojo, C. Murakami, A. Fuji and A. Hosomi, *Tetrahedron Lett.,* 1999, **40**, 911–914; (h) F. Le Bideau, T. Caradin, D. Gourier, J. Hénique and E. Samuel, *Tetrahedron Lett.,* 2000, **41**, 5215–5218; (i) J. Boyer, R. J. P. Corriu, R. Perz and C. Reye, *J. Organomet. Chem.,* 1979, **172**, 143–152; (j) J. Boyer, R. J. P. Corriu, R. Perz, M. Poirier and C. Reye, *Synthesis,* 1981, 558–559; (k) D. Yang and D. D. Tanner, *J. Org. Chem.,* 1986, **51**, 2267–2270; (l) M. Fujita and T. Hiyama, *J. Org. Chem.* 1988, **53**, 5405–5415; (m) C. Chuit, R. J. P. Corriu and J. C. Young, *Chem. Rev.,* 1993, **93**, 1371–1448; (n) Y. Kobayashi, E. Takahisa, M. Akano and K. Watatani, *Tetrahedron,* 1997, **53**,

View Article Online
DOI: 10.1039/C7DT04858K

1627–1634; (o) Y. Kawanami, H. Yuasa, F. Toriyama, S. Yoshida and T. Baba, *Catal. Commun.* 2003, **4**, 455–459.

6. (a) M. Pérez, Z.-W. Qu, C. B. Caputo, V. Podgorny, L. J. Hounjet, A. Hansen, R. Dobrovetsky, S. Grimme and D. W. Stephan, *Chem. Eur. J.,* 2015, **21**, 6491–6500; (b) J. H. W. LaFortune, T. C. Johnstone, M. Pérez, D. Winkelhaus, V. Podgorny and D. W. Stephan, *Dalton Trans.,* 2016, **45**, 18156–18162.

7. J. Chen, L. Falivene, L. Caporaso, L. Cavallo and E. Y.-X. Chen, *J. Am. Chem. Soc.* 2016, **138**, 5321−5333.

8. (a) D. J. Parks, J. M. Blackwell and W. E. Piers, *J. Org. Chem.,* 2000, **65**, 3090–3098; (b) D. J. Parks and W. E. Piers, *J. Am. Chem. Soc.,* 1996, **118**, 9440–9441; (c) R. Roesler, B. J. N. Har and W. E. Piers, *Organometallics,* 2002, **21**, 4300–4302; (d) J. M. Blackwell, D. J. Morrison and W. E. Piers, *Tetrahedron*, 2002, **58**, 8247–8254; (e) J. Hermeke, M. Mewald, and M. Oestreich, *J. Am. Chem. Soc.* 2013, **135**, 17537–17546; (f) J. M. Blackwell, E. R. Sonmor, T. Scoccitti and W. E. Piers, *Org. Lett.* 2000, **2**, 3921–3923.

9. (a) S. Rendler and M. Oestreich, *Angew. Chem. Int. Ed.,* 2008, **47**, 5997–6000; (b) D. Hog, M. Oestreich, *Eur. J. Org. Chem.* 2009, 5047–5056.

10. (a) H. Braunschweig, A. Damme, C. Hörl, T. Kupfer and J. Wahler, *Organometallics,* 2013, **32**, 6800–6803. (b) A. Y. Houghton, J. Hurmalainen, A. Mansikkamäki, W. E. Piers and H. M. Tuononen, *Nat. Chem.,* 2014, **6**, 983–988. (c) V. Varga, M. Lamač, M. Horáček, R Gyepes and J. Pinkas, *Dalton Trans*., 2016, **45**, 10146–10150.

11. J. Chen, L. Falivene, L. Caporaso, L. Cavallo and E. Y.-X. Chen, *J. Am. Chem. Soc.* 2016, **138**, 5321−5333.

12. (a) A. Brzozowska, P. Ćwik, K. Durka, T. Kliś, A. E. Laudy, S. Luliński, J. Serwatowski, S. Tyski, M. Urban and W. Wróblewski, *Organometallics,* 2015, **34**, 2924–2932; (b) I. Steciuk, K. Durka, K. Gontarczyk, M. Dąbrowski, S. Luliński and K. Woźniak, *Dalton Trans.* 2015, **44**, 16534–16546.

13. M. Czub, K. Durka, S. Luliński, J. Łosiewicz, J. Serwatowski, M. Urban and K. Woźniak, *Eur. J. Org. Chem.* 2017, 818–828.

14. A. Kawachi, M. Zaima and Y. Yamamoto, *Organometallics* 2008, **27**, 4691−4696.

15. A. Kawachi, H. Morisaki, N. Nishioka and Y. Yamamoto, *Chem. Asian J.* 2012, **7**, 546–553.

16. D. J. Parks, R. E. von H. Spence and W. E. Piers, *Angew. Chem. Int. Ed.,* 1995, **34**, 809–811.

17. For related preceding studies on the topic, see: (a) L. S. Chen, G. J. Chen and C. Tamborski, *J. Organomet. Chem.* 1980, **193**, 283–292; (b) A. Kawachi, M. Zaima, A. Tani and Y. Yamamoto, *Chem. Lett.,* 2007, **36**, 362–363; (c) A. Kawachi, *J. Synth. Org. Chem. Jpn,* 2017, **75**, 714–722.

18. P. F. Hudrlik, A. M. Hudrlik and Y. A. Jeilani, *Tetrahedron,* 2011, **67**, 10089–10096.

19. X.-H. Chen, Y. Deng, K. Jiang, G.-Q. Lai, Y. Ni, K.-F. Yang, J.-X. Jiang and L.-W. Xu, *Eur. J. Org. Chem.,* 2011, 1736–1742.

20. For some analogy, see: K. Durka, T. Kliś, J. Serwatowski and K. Woźniak, *Organometallics*, 2013, **32**, 3145−3148.

View Article Online
DOI: 10.1039/C7DT04858K

21. M. Shindo, K. Matsumoto and K. Shishido, *Angew. Chem. Int. Ed.,* 2004, **43**, 104–106.
22. Y. Zhao and D. G. Truhlar, *Theor. Chem. Acc.,* 2008, **120**, 215–41.
23. (a) R. Krishnan, J. S. Binkley, R. Seeger and J. A. Pople, *J. Chem. Phys.,* 1980, **72**, 650−654; (b) C. Lee, W. Yang and R. G. Parr, *Phys. Rev. B,* 1988, **37**, 785–789.
24. M. J. Frisch, G. W. Trucks, H. B. Schlegel, G. E. Scuseria, M. A. Robb, J. R. Cheeseman, J. A. Montgomery, Jr., T. Vreven, K. N. Kudin, J. C. Burant, J. M. Millam, S. S. Iyengar, J. Tomasi, V. Barone, B. Mennucci, M. Cossi, G. Scalmani, N. Rega, G. A. Petersson, H. Nakatsuji, M. Hada, M. Ehara, K. Toyota, R. Fukuda, J. Hasegawa, M. Ishida, T. Nakajima, Y. Honda, O. Kitao, H. Nakai, M. Klene, X. Li, J. E. Knox, H. P. Hratchian, J. B. Cross, V. Bakken, C. Adamo, J. Jaramillo, R. Gomperts, R. E. Stratmann, O. Yazyev, A. J. Austin, R. Cammi, C. Pomelli, J. W. Ochterski, P. Y. Ayala, K. Morokuma, G. A. Voth, P. Salvador, J. J. Dannenberg, V. G. Zakrzewski, S. Dapprich, A. D. Daniels, M. C. Strain, O. Farkas, D. K. Malick, A. D. Rabuck, K. Raghavachari, J. B. Foresman, J. V. Ortiz, Q. Cui, A. G. Baboul, S. Clifford, J. Cioslowski, B. B. Stefanov, G. Liu, A. Liashenko, P. Piskorz, I. Komaromi, R. L. Martin, D. J. Fox, T. Keith, M. A. Al-Laham, C. Y. Peng, A. Nanayakkara, M. Challacombe, P. M. W. Gill, B. Johnson, W. Chen, M. W. Wong, C. Gonzalez and J. A. Pople, *Gaussian09*, Gaussian, Inc.: Wallingford, CT, 2010.
25. (a) J. C. Sheldon, R. N. Hayes and J. H. Bowie, *J. Am. Chem. Soc.*, 1984, **106**, 7711–7715; (b) C. H. DePuy, V. M. Bierbaum, L. A. Flippin, J. J. Grabowski, G. K. King, R. J. Schmitt and S. A. Sullivan, *J. Am. Chem. Soc.,* 1980, **102**, 5012–5015; (c) J. C. Sheldon, R. N. Hayes, J. H. Bowie and C. H. DePuy, *J. Chem. Soc., Perkin Trans. II*, 1987, 275–280.
26. (a) F. Effenberger and W. Daub, *Chem. Ber.*, 1991, **124**, 2113–2118; (b) F. Effenberger and W. Daub, *Chem. Ber.*, 1991, **124**, 2119–2125.
27. CrysAlis Pro Software; Oxford Diffraction Ltd.: Oxford, U.K., 2010.
28. G. M. Sheldrick, *Acta Crystallogr.* 2008, **A64**, 112–122.
29. G. M. Sheldrick, *Acta Crystallogr.* 2015, **C71**, 3–8.
30. (a) E. Canses, B. Mennucci and J. Tomasi, *J. Chem. Phys.*, 1997, **107**, 3032–3041; (b) J. Tomasi and M. Persico, *Chem. Rev.,* 1994, **94**, 2027–2094; (c) J. Tomasi, B. Mennucci and R. Camm, *Chem. Rev.,* 2005, **105**, 2999–3093.